Supporting Information

Kinetics of Dehydrogenation of *n*-Heptane over Ga-Pt Supported Catalytically Active Liquid Metal Solutions (SCALMS)

Oshin Sebastian,[1] Asem Al-Shaibani,[1] Nicola Taccardi,[1] Marco Haumann,[1,2*] Peter Wasserscheid,[1,3*]

1 Friedrich-Alexander-Universität Erlangen-Nürnberg (FAU), Lehrstuhl für Chemische Reaktionstechnik (CRT), Egerlandstraße 3, 91058 Erlangen, Germany

2 Research Centre for Synthesis and Catalysis, Department of Chemistry, University of Johannesburg, P.O. Box 524, Auckland Park 2006, South Africa

3 Forschungszentrum Jülich GmbH, Helmholtz-Institute Erlangen-Nürnberg for Renewable Energy (IEK 11), Egerlandstraße 3, 91058 Erlangen, Germany

*Corresponding author e-mail address: marco.haumann@fau.de; peter.wasserscheid@fau.de

Literature survey – kinetic parameters for *n*-heptane conversion reaction

Table S1: Kinetic data for *n*-heptane conversion over Pt-based catalysts available in literature to date.

Catalyst	**Reaction**	**P** bara	**T** °C	**$E_{A,app.}$** kJ mol^{-1}	**H_2 order** -	**Hep order** -	**Ref.**
Pt/Al_2O_3	Reform.	4	420-500	30-42	-	-	[1]
1.0% Pt/Al_2O_3	Reform.	1	285-420	80	-	-	[2]
0.3% Pt/Al_2O_3	Reform.	1	285-420	83	-	-	[2]
0.6% Pt/Al_2O_3	Isom.	3-21	285-465	88	-	-	[3]
0.6% Pt/Al_2O_3	Crack.	3-21	285-465	256	-	-	[3]
0.6% Pt/Al_2O_3	Cycl.	3-21	285-465	256	-	-	[3]
Pt/Al_2O_3	Dehydro.	-	-	76 (DFT)	-	-	[4]
1.0% Pt-0.3%Sn/Al_2O_3	Reform.	1	285-420	116	-	-	[2]
0.3% Pt-0.3%Sn/Al_2O_3	Reform.	1	285-420	196	-	-	[2]
0.3% Pt 1.0%Sn/Al_2O_3	Reform.	1	285-420	146	-	-	[2]
Pt-Re/Al_2O_3	Cycl.	5	460-520	132	-	-	[5]
Pt-Re/Al_2O_3	Arom.	5	460-520	72	-	-	[5]
Pt-Re/Al_2O_3	Isom.	5	460-520	10	-	-	[5]
Pt-Re/Al_2O_3	Crack.	5	460-520	109	-	-	[5]
Pt-Re/Al_2O_3	Arom.	50	460-520	153	-	-	[6]
0.3% Pt-0.3%Re/Al_2O_3	Isom.	4-17	350-500	201	-	-	[7]
0.3% Pt-0.3%Re/Al_2O_3	Crack.	4-17	350-500	241	-	-	[7]
0.3% Pt-0.3%Re/Al_2O_3	Cycl.	4-17	350-500	454	-	-	[7]
Pt/H-Y	Isom.	1	195-240	94	-	-	[8]
Pt-Zn/H-Y	Isom.	1	195-240	143	-	-	[8]
1.0% Pt/USY	Isom.	1-15	210-250	94-108	-0.23 to -0.02	-0.32 to -0.11	[9]
2.0% Pt/USY	Isom.	1-15	210-250	103	~0	-0.08	[9]
1.0% Pt/Beta	Isom.	1-15	210-250	107-133	-0.34 to -0.20	-0.44 to -0.08	[9]
0.2%Pt/S-Zr	Isom. & crack.	1-4	150-250	77-132	-0.50 to -0.15 (LP) 0 to 0.8 (HP)	0.95-1.0	[10]
Pt-Sn/ZH	Isom.	1	200-350	33	-1.76 to -0.35	0.30 to 0.88	[11]
Pt-Re/ZH	Isom.	1	200- 350	77	-0.54 to 0.10	0.20 to 1.0	[11]
Pt-Sn-Re/ZH	Isom.	1	200-350	55	-0.21 to 0.02	0.15 to 0.54	[11]
Pt-Re-Sn/ZH	Isom.	1	200-350	65	-0.08 to 0	0.12 to 0.63	[11]
Pt/HMOR	Isom.	5-40	180-220	118	-1.08	0.15	[12]
Pt/Zr-HMS	Reform.	1	200-500	10-12	-	-	[13]
Pt/Zr-HMS	Reform.	1	200-500	10-12	-	-	[13]
0.5%Pt/H-ZSM5	Crack.	0-22	235-275	84 (no H_2) 178	- -		[14]
1.0 %Pt/H-Y	Isom.	1.1	175-185	125-142	-	-	[15]
0.3% Pt/SO_x-ZrO_2	Isom.	31	200	-	1	0.2	[16]

Reform. = reforming; Isom. = isomerization or hydroisomerization; Crack. = cracking or hydrocracking; Cycl. = cyclization or hydrocyclization; Dehydro. = dehydrogenation; P = pressure; T = temperature; $E_{A,app}$ = apparent activation energy; DFT = density functional theory; HY = HY zeolite; USY = ultra-stable Y zeolite; Beta = beta structured zeolite (CP814C); S-Zr = sulfated zirconia; HMOR = hydrogen mordenite; HMS = hexagonal mesoporous silica; Zr-HMS

= zirconia containing hexagonal mesoporous silica; HZSM-5 = H form of ZSM-5 zeolite; HY = H form of Y-type zeolite; LP = low H_2 partial pressure (0.25-1.0 bar); HP = high H_2 partial pressure (1.2-4.0 bar)

Gas-phase dehydrogenation set-up

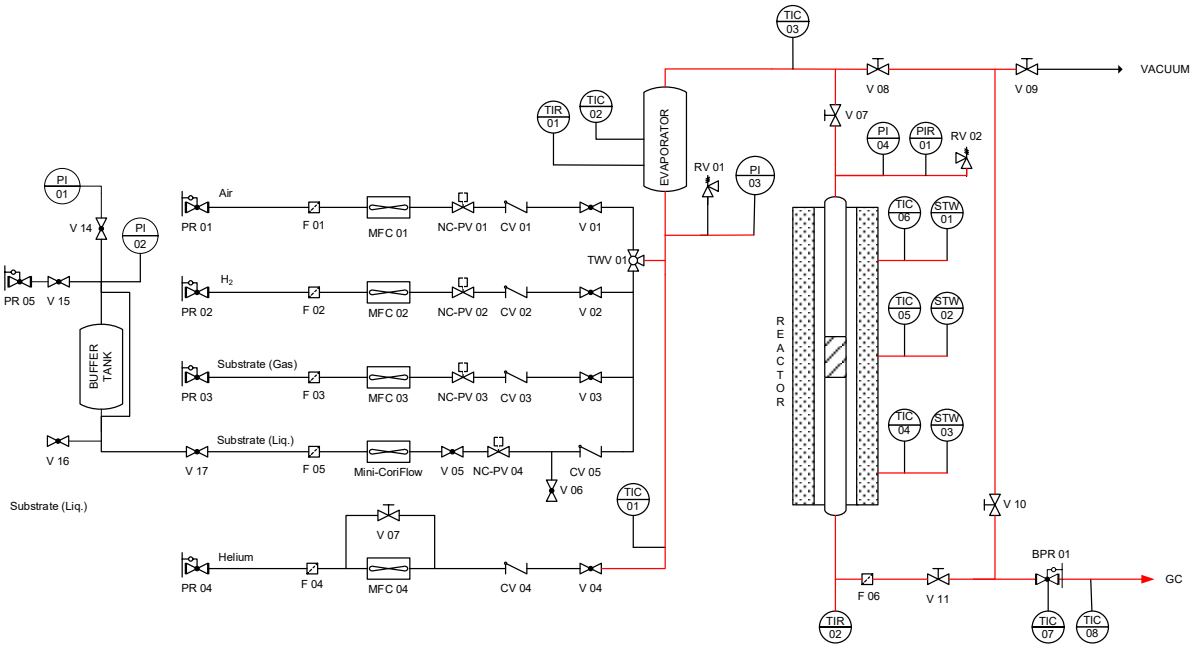

Figure S1: Flow scheme of the continuous gas-phase reactor set up for *n*-heptane dehydrogenation. Heated lines are shown in red.

Figure S2: Image of gas-phase reactor setup used for *n*-heptane dehydrogenation.

Reaction product analysis

A sample of gas chromatograph showing the separation and detection of various products formed in *n*-heptane dehydrogenation is shown in Figure S3.

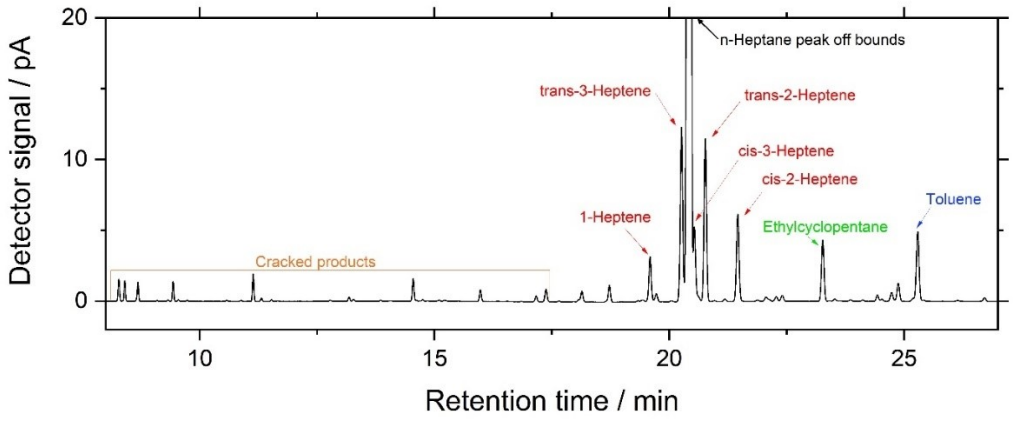

Figure S3: Representative GC chromatogram showing products separation and detection in *n*-heptane dehydrogenation.

The summary and classification of the different species that were identified by means of GC analysis is shown Table S2.

Table S2: Reaction products detected in *n*-heptane dehydrogenation at 703 K under atmospheric pressure.

Products	**Classification**	**Relevant reactions**
Methane, ethane, ethane, propane, propene, cyclopentane, methylcyclopentane, 2-methylpetane, 3-methylpentane, hexane, benzene,	Cracked products (≤ C6)	Hydrocracking Hydrogenolysis
n-heptane	C7 *n*-alkane	
1-heptene, *trans*-2-heptene, *cis*-2-heptene, *trans*-3-heptene, *cis*-3-heptene	C7 *n*-alkenes	Dehydrogenation
2,2-dimethylpentane, 3,3-dimethylpentane, 2,3-dimethylpentane, 2-methylhexane, 3-methylhexane	C7 *iso*-alkanes	Isomerization
5-methyl-1-hexene, 3-ethyl-2-pentene, 3-methyl-2-hexene, 2-methyl-2,4-hexadiene, 2,3-dimethyl-1,3-pentadiene	C7 *iso*-alkenes	Dehydrogenation-isomerization
Cis-1,3-dimethylcyclopentane, *trans*-1,3-dimethylcyclopentane, 1,2-dimethylcyclo-pentane, methylcyclohexane, ethylcyclopentane	C7 sub.-cyclo-alkanes	Cyclization
3,5-dimethylcyclopentene, 1-ethylcyclopentene	C7 sub.-cyclo-alkenes	Dehydrocyclization
Toluene	C7 aromatics	Aromatization

Note: sub.-cyclo = substituted cyclic

Since the number of dehydrogenated species within the fractions of isomerized and cyclized compounds was very small (< 1%), they were included in the lumped model. Hence, only six compound classes were discussed, i.e., < C6 cracking, desired *n*-heptene, isomerized C7, C7 cyclics, C7 aromatics and unspecified.

The conversion of *n*-heptane X_i, the product selectivity S_p, and the product yield Y_p is calculated as follows:

Conversion of *n*-heptane, $$X_i = \frac{x_{i,0} - x_i}{x_{i,0}} \quad \text{(S1)}$$

Selectivity of products, $$S_p = \frac{x_p}{x_{i,0} - x_i} \quad \text{(S2)}$$

Yield of products, $$Y_p = X_i * S_p \quad \text{(S3)}$$

n-Heptene productivity, $$P_k = \frac{F_i * X_i * S_k}{m_{Pt}} \quad \text{(S4)}$$

Overall rate of reaction, $$r = \frac{X_i \cdot F_i}{m_{pt}} \quad \text{(S5)}$$

Where $x_{i,0}$ is the mole fraction of *n*-heptane in the feed, x_i is the mole fraction of *n*-heptane in the product stream, x_p is the mole fraction of product, F_i is the mole flow rate of *n*-heptane in the feed, S_k is the selectivity towards *n*-heptenes, and m_{Pt} is the mass of Pt in the catalyst bed.

Equilibrium conversion – dehydrogenation of *n*-heptane to *n*-heptenes

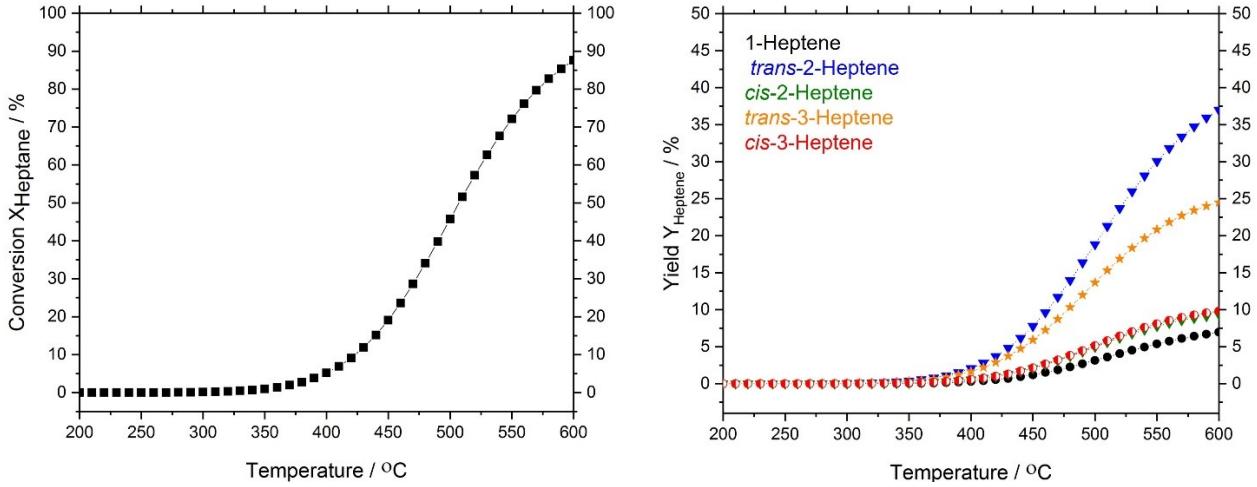

Figure S4: Equilibrium conversion of *n*-heptane to *n*-heptene isomers (under atmospheric conditions).

Catalysts tested in *n*-heptane dehydrogenation

Table S3: Overview of catalysts and their compositions tested in this study.

Catalyst ID	Catalyst composition	Pt	Ga	Ga/Pt
		wt.%	wt.%	mol/mol
AA006	Pt/Al_2O_3	0.12	-	-
AA007	Pt/Al_2O_3	0.09	-	-
TN861	$Ga\text{-}Pt/Al_2O_3$	0.08	2.4	84

Catalytic results

Bare Al_2O_3 support activity in *n*-heptane dehydrogenation

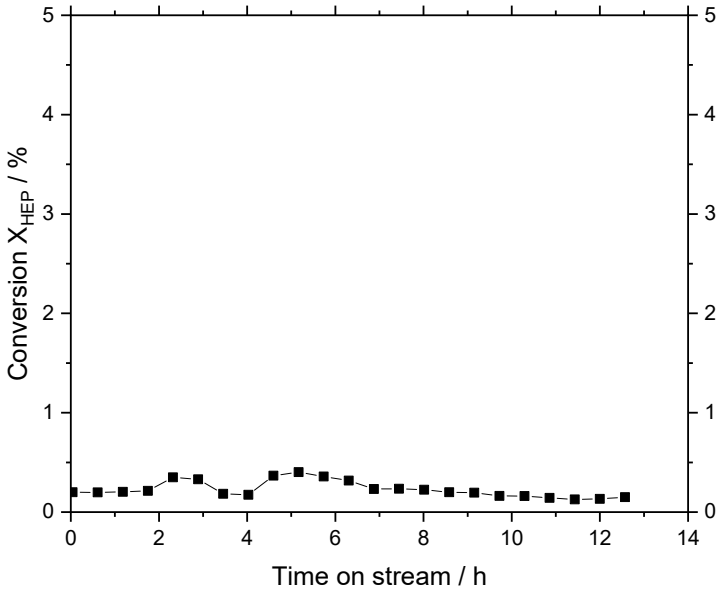

Figure S5: Graph showing conversion over time-on-stream in *n*-heptane dehydrogenation using bare Al_2O_3 support. Reaction conditions: 703 K, atmospheric pressure, 2.5 mL catalyst bed volume, 150 ml_N min^{-1} total flow, H_2/heptane = 8, 100 mbar *n*-heptane, 800 mbar H_2, and 100 mbar He.

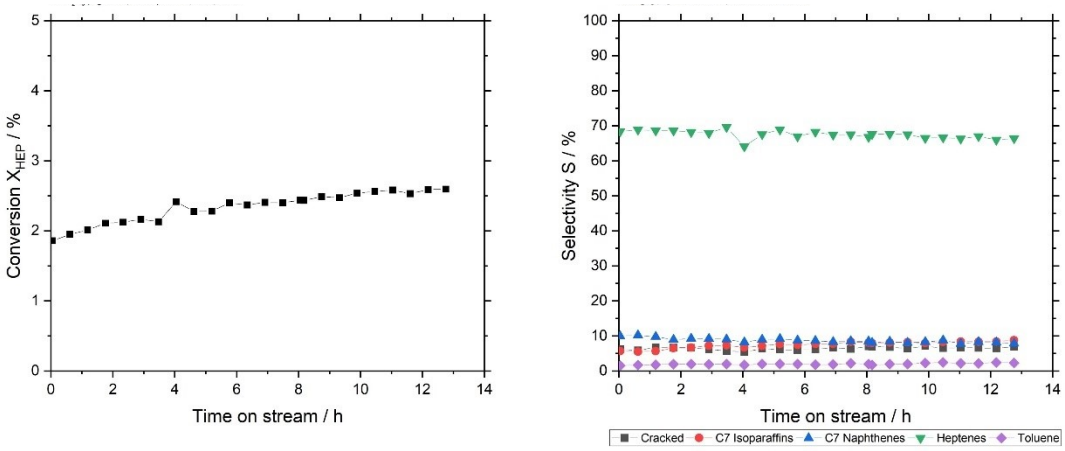

Figure S6: Graph showing conversion over time-on-stream in *n*-heptane dehydrogenation using Ga/Al_2O_3 material. Reaction conditions: 703 K, atmospheric pressure, 2.5 mL catalyst bed volume, 150 ml_N min^{-1} total flow, H_2/heptane = 8, 100 mbar *n*-heptane, 800 mbar H_2, and 100 mbar He.

Variation of support particle size at constant residence time

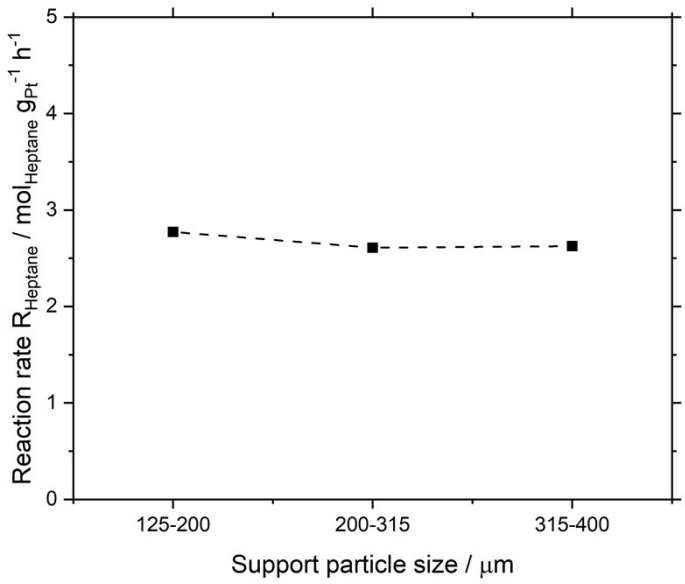

Figure S7: Variation of support particle size in *n*-heptane dehydrogenation using Pt/Al_2O_3 catalyst. Pre-reduction conditions: 723 K, atmospheric pressure, 50 $mL_N min^{-1}$ H_2 flow, 120 min. Reaction conditions: 743 K, atmospheric pressure, 3.5 mL catalyst bed volume, 150 ml_N min^{-1} total flow, H_2/heptane = 8, 100 mbar *n*-heptane, 800 mbar H_2, and 100 mbar He.

Variation of total volumetric flow at constant residence time

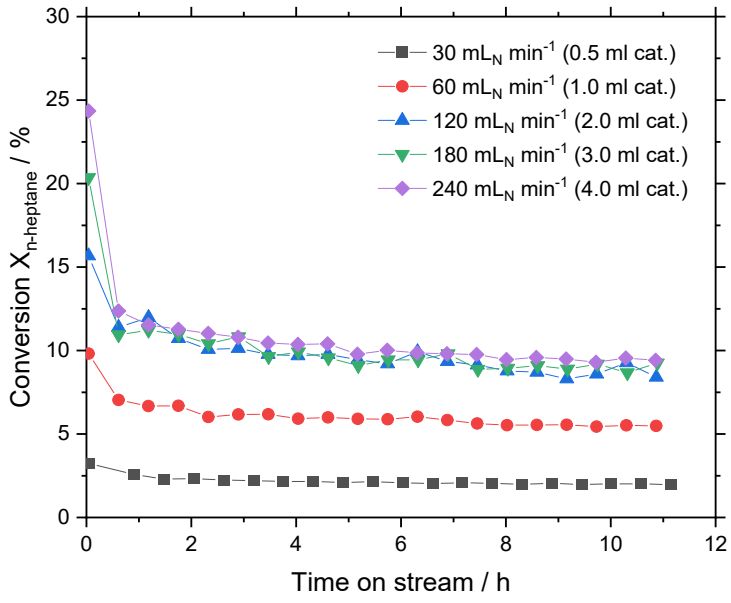

Figure S8: Variation of total volumetric flow at constant residence time in *n*-heptane dehydrogenation using Pt/Al_2O_3 catalyst. Pre-reduction conditions: 723 K, atmospheric pressure, 50 $mL_N min^{-1}$ H_2 flow, 120 min. Reaction conditions: 743 K, atmospheric pressure, 0.5-4.0 mL catalyst bed volume, 30-240 ml_N min^{-1} total flow, H_2/heptane = 5, 100 mbar *n*-heptane, 500 mbar H_2, and 400 mbar He.

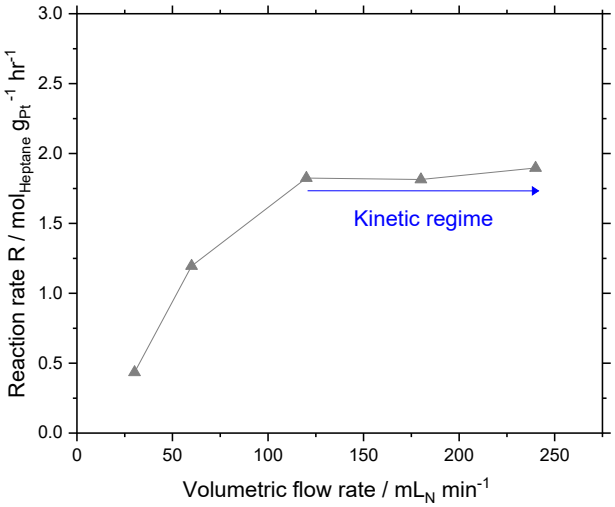

Figure S9: Variation of total volumetric flow at constant residence time in *n*-heptane dehydrogenation using Pt/Al_2O_3 catalyst. Pre-reduction conditions: 723 K, atmospheric pressure, 50 $mL_N min^{-1}$ H_2 flow, 120 min. Reaction conditions: 743 K, atmospheric pressure, 0.5-4.0 mL catalyst bed volume, 30-240 ml_N min^{-1} total flow, 100 mbar *n*-heptane, 500 mbar H_2, and 400 mbar He.

Productivity for Pt/Al_2O_3 and $Ga_{84}Pt/Al_2O_3$

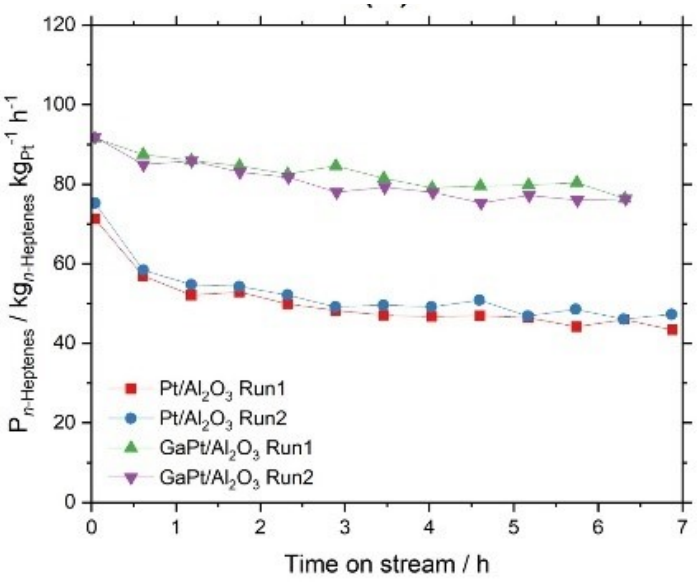

Figure S10. *n*-Heptene productivity of Pt/Al_2O_3 and $Ga\text{-}Pt/Al_2O_3$ (SCALMS) in *n*-heptane dehydrogenation. Pre-reduction conditions: 723 K, atmospheric pressure, 50 $mL_N min^{-1}$ H_2 flow, 120 min. Reaction conditions: 703 K, atmospheric pressure, 2.5 mL catalyst bed volume, 150 ml_N min-1 total flow, 100 mbar *n*-heptane, 200 mbar H_2, and 700 mbar He.

H_2 reaction order experiments

Table S4: Summary of catalytic results of H_2 reaction order determination experiments at 703 K, atmospheric pressure, 2.5 mL catalyst bed volume, 150 ml_N min-1 total flow, 100 mbar *n*-heptane, 200-800 mbar H_2, and 100-700 mbar He.

Catalyst	H_2	$X_{n\text{-}heptane}$	$S_{n\text{-}heptenes}$	$S_{cracked}$	$S_{Toluene}$	$Y_{n\text{-}heptenes}$	$Y_{cracked}$	$Y_{Toluene}$
	mbar	%	%	%	%	%	%	%
Pt/Al_2O_3	200	5.7%	78.0%	3.8%	3.7%	4.4%	0.2%	0.2%
	400	6.1%	77.8%	4.7%	4.4%	4.7%	0.3%	0.3%
	600	6.3%	75.6%	7.0%	4.1%	4.8%	0.4%	0.3%
	800	8.1%	64.2%	10.0%	7.0%	5.2%	0.8%	0.6%
SCALMS	200	6.0%	79.9%	2.6%	3.2%	4.8%	0.2%	0.2%
	400	6.1%	80.7%	4.1%	3.2%	4.9%	0.3%	0.2%
	600	6.5%	74.5%	5.7%	4.0%	4.8%	0.4%	0.3%
	800	6.6%	71.9%	5.8%	4.4%	4.7%	0.3%	0.4%

n-Heptane reaction order experiments

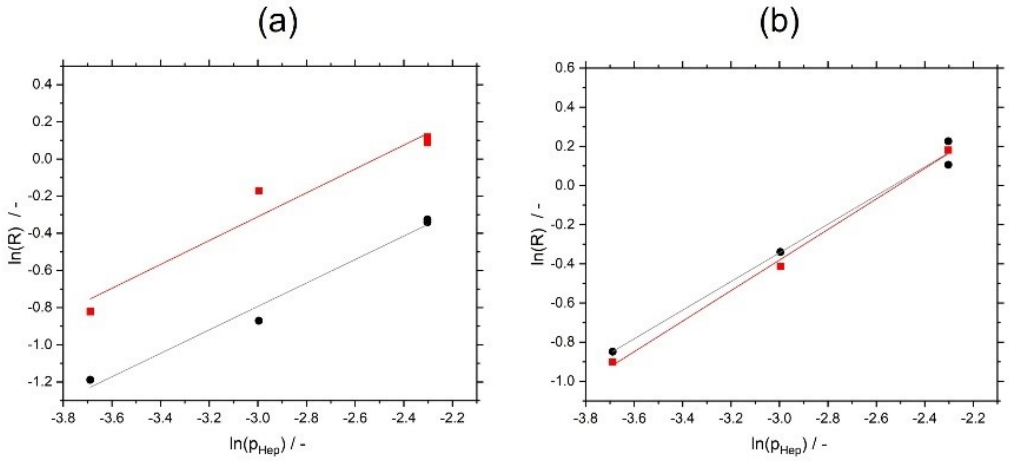

Figure S11: *n*-heptane reaction order: Logarithmic plot of reaction rate of *n*-heptane dehydrogenation as a function of *n*-heptane partial pressure at (a) 200 mbar and (b) 800 mbar constant H_2 partial pressure for SCALMS (red squares ■) and Pt/Al_2O_3 (black circles ●). Pre-reduction conditions: 723 K, atmospheric pressure, 50 $mL_N min^{-1}$ H_2 flow, 120 min. Reaction conditions: 703 K, atmospheric pressure, 2.5 mL catalyst bed volume, 150 ml_N min-1 total flow, 25-100 mbar *n*-heptane, 200 or 800 mbar H_2, and 100-775 mbar He.

Table S5: Summary of catalytic results of *n*-heptane reaction order (at 200 mbar H_2) determination experiments at 703 K, atmospheric pressure, 2.5 mL catalyst bed volume, 150 ml_N min-1 total flow, , 25-100 mbar *n*-heptane, 200 mbar H_2, and 100-775 mbar He.

Catalyst	***n*-Heptane** mbar	$X_{n\text{-}heptane}$ %	$S_{n\text{-}heptenes}$ %	$S_{cracked}$ %	$S_{Toluene}$ %	$Y_{n\text{-}heptenes}$ %	$Y_{cracked}$ %	$Y_{Toluene}$ %
Pt/Al_2O_3	25	10.0%	69.9%	8.3%	7.5%	7.0%	0.8%	0.8%
	50	6.6%	76.5%	5.2%	4.8%	5.1%	0.3%	0.3%
	100	5.7%	78.0%	3.8%	3.7%	4.4%	0.2%	0.2%
SCALMS	25	9.8%	67.5%	5.9%	7.7%	6.6%	0.6%	0.8%
	50	9.1%	69.6%	4.5%	7.2%	6.3%	0.4%	0.7%
	100	6.0%	79.9%	2.6%	3.2%	4.8%	0.2%	0.2%

Table S6: Summary of catalytic results of *n*-heptane reaction order (at 800 mbar H_2) determination experiments at 703 K, atmospheric pressure, 2.5 mL catalyst bed volume, 150 ml_N min-1 total flow, , 25-100 mbar *n*-heptane, 800 mbar H_2, and 100-175 mbar He.

Catalyst	***n*-Heptane** mbar	$X_{n\text{-}heptane}$ %	$S_{n\text{-}heptenes}$ %	$S_{cracked}$ %	$S_{Toluene}$ %	$Y_{n\text{-}heptenes}$ %	$Y_{cracked}$ %	$Y_{Toluene}$ %
Pt/Al_2O_3	25	10.5%	49.1%	19.0%	11.2%	5.2%	2.0%	1.2%
	50	8.5%	61.6%	12.7%	7.9%	5.2%	1.1%	0.7%
	100	8.8%	64.5%	9.9%	7.1%	5.7%	0.9%	0.6%
SCALMS	25	8.6%	56.1%	13.0%	9.0%	4.8%	1.1%	0.8%
	50	7.2%	63.0%	8.5%	6.3%	4.5%	0.6%	0.5%
	100	6.6%	71.9%	5.8%	4.4%	4.7%	0.3%	0.4%

Product yield at different temperatures

Table S7: Summary of conversion and productivity of SCALMS and Pt/Al_2O_3 catalyst in *n*-heptane dehydrogenation. Pre-reduction conditions: 723 K, atmospheric pressure, 50 $mL_N min^{-1}$ H_2 flow, 120 min. Reaction conditions: 683-743 K, atmospheric pressure, 2.5 mL catalyst bed volume, 150 ml_N min-1 total flow, 100 mbar *n*-heptane, 800 mbar H_2, and 100 mbar He.

Catalyst	Temperature	Conversion	Productivity
	K	%	$g_{n-heptene} g_{Pt}^{-1} h^{-1}$
SCALMS	683	3.9	51
	703	7.8	124
	723	8.2	97
	743	9.3	94
Pt/Al_2O_3	683	4.8	43
	703	7.1	65
	723	9.8	86
	743	35.0	83

Evaluation of kinetic data

The reaction rate r for *n*-heptane dehydrogenation in presence of added H_2 can be written in general form following the power-law model as,

$$r = k * p(H_2)^n * p(Hep)^m \quad \text{(S6)}$$

where k is the reaction rate constant, "$p(H_2)$" is the partial pressure and "n" is the reaction order of H_2, and "$p(Hep)$" is the partial pressure and "m" is the reaction order of *n*-heptane.

The reaction rate constant here relates the rate of the reaction to temperature and is given by Arrhenius law.

$$k = k_0 \, e^{-\frac{E_a}{RT}} \quad \text{(S7)}$$

where k_0 is the pre-exponential factor and has units of s^{-1}, E_a is the activation energy in $J\,mol^{-1}$ units, R is the universal gas constant, and T is the temperature in K units.

Experimentally, the reaction order is identified by a variation of the partial pressure of a given species, then plotting the natural logarithm of the reaction rate versus the natural logarithm of the partial pressure. The slope of the linear fit in this plot is equal to the reaction order of the varied species.

For example, for the determining the reaction order of H_2, the Equation S5 can be modified to

$$\ln(r) = \ln\left[k\, p(Hep)^m\right] + n * \ln p(H_2) \tag{S8}$$

The reaction order of H_2 (i.e., n) can then be calculated by finding the slope of the regression line.

Likewise, the activation energy is formally expressed as

$$E_a = -R\frac{\partial \ln k}{\partial(1/T)} \tag{S9}$$

This is determined experimentally by varying the temperature while maintaining constant operating conditions. It is useful to use the reaction rate directly by substituting Equation S6 in S5.

$$\ln(r) = \ln\left[k_0 * p(H_2)^n * p(Hep)^m\right] - \frac{E_a}{R}\left(\frac{1}{T}\right) \tag{S10}$$

Plotting the natural logarithm of the reaction rate versus $1/T$ would yield a linear line with $-\frac{E_A}{R}$ as its slope.

Alternatively, Equation S9 can be rearranged to allow the determination of the pre-exponential factor (k_0) as the intercept of the y-axis, such that

$$\ln\left(\frac{r}{P(H_2)^n * P(Hep)^m}\right) = \ln(k_0) - \frac{E_a}{R}\left(\frac{1}{T}\right) \tag{S11}$$

It is important to note that the power-law parameters are dependent on the operating conditions and are calculated for the specific operating range at which they were determined.

Parameter fitting (using MATLAB)

A minimization algorithm was employed to fit the power-law model parameters, namely pre-exponential factor (k_0), reaction orders (n & m), and activation energy (E_a). The two-step minimization algorithm uses two different mathematical approaches for the fitting of the data. Both mathematical methods are part of the MATLAB optimization toolbox. The first step of the minimization algorithm is the fitting of each parameter independently from other parameters using a nonlinear least-squares solver. The next step is a final minimization for all parameters simultaneously using a non-linear multi-variable function solver that employs an interior-point algorithm.

The minimization function employs the sum of squared errors (SSE) as the objective function to be minimized. The SSE function calculates the error between the experimental value and the calculated value from the estimated parameter (see Equation S11)

$$SSE = \sum_{i=1}^{N}\left(R_{experimental,i} - R_{calculated,i}\right)^2 \tag{S12}$$

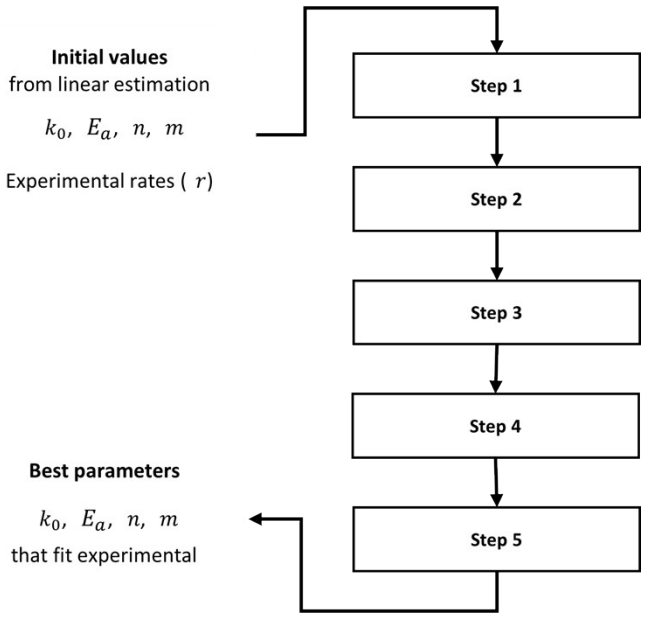

Figure S12: MATLAB minimization algorithm: Each parameter is fitted independently, and then in the final step, all the parameters are refitted to reduce the sum of squared errors (SSE) further. The algorithm uses linear estimates from the graphical method as inputs in addition to experimental parameters and boundary conditions. Boundary conditions include a positive value for activation energy, for example.

CO – temperature programmed desorption

CO-temperature programmed desorption (CO-TPD) experiments were carried out on a Micromeritics Autochem II 2920 Chemisorb. 0.2 – 0.3 g of sample was *in situ* reduced in 20% H_2 in Ar mixture for 2 h at 200°C and then flushed with 99.999% He for 1 h at 200°C to obtain a clean surface. Then, the sample was cooled to 40°C and allowed to adsorb CO for 2 h. After that, the sample was flushed with He until the baseline was stable. Finally, the temperature was elevated at a rate of 5°C min^{-1} from 40 °C to 200°C in He flow. The desorbed CO was detected by TCD. All results were normalized to the weight of the sample.

The dispersion is calculated using the equation S13 shown below.

$$Pt\ disperson, D = 100\% * \frac{n_{CO,\ adsorbed}}{n_{Pt}} \quad \text{(S13)}$$

$n_{CO,\ adsorbed}$ = moles of CO adsorbed on sample, which is calculated from the volume of the dosed CO minus non-adsorbed CO (i.e., desorbed CO).

n_{Pt} = moles of Pt in the sample, which is calculated from the sample mass used and Pt loading in the sample (determined by ICP-AES).

Table S8: Results of CO-temperature programmed desorption (CO-TPD) experiments of catalysts in this study.

Sample	**CO adsorbed** μmol g^{-1}	**Dispersion** %
Pt/Al_2O_3 (Pt=0.12 wt.%)	0.165	1.84
Ga/Al_2O_3 (Ga = 2.83 wt.%)	0	0
$Ga_{88}Pt/Al_2O_3$ (Ga = 2.83 wt.%, Pt=0.09 wt.%)	0.108	2.35

Exemplary workflow (H_2 reaction order determination

This section shows the reader an exemplary standard workflow used for determination of reaction order of H_2.

Firstly, the conversion of the Ga-Pt/AlOx SCALMS as well as Pt/AlOx were determined at various partial pressure of H_2 while keeping the n-heptane partial pressure constant. Figure S13 shows exemplary data obtained for Ga-Pt/AlOx SCALMS and Pt/AlOx with a H_2 partial pressure of 200 mbar and *n*-heptane partial pressure of 100 mbar at 703 K and atmospheric pressure.

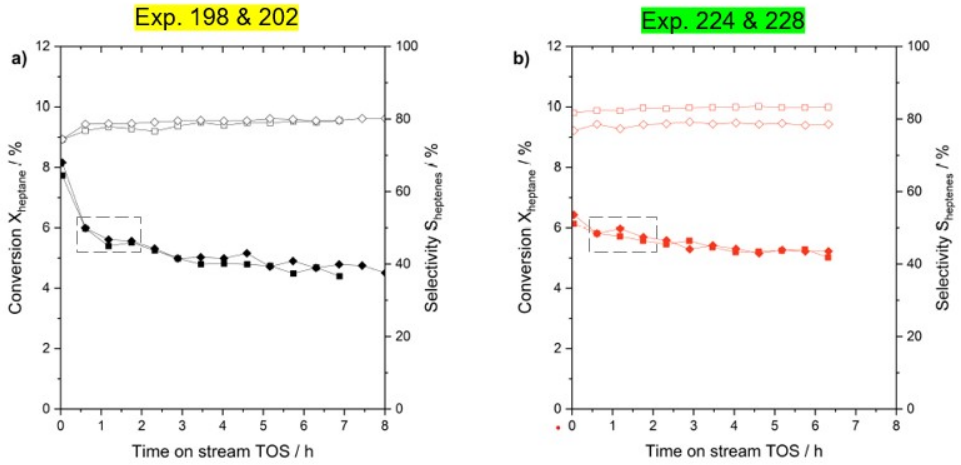

Exp.	Catalyst	Avg. Conversion* (%)
198	Pt/AlOx (Pt = 0.12 wt.%)	5.63 %
202	Pt/AlOx (Pt = 0.12 wt.%)	5.72 %
224	Ga-Pt/AlOx (Pt = 0.08 wt.%)	5.89%
228	Ga-Pt/AlOx (Pt = 0.08 wt.%)	6.07%

*Average of 3 consecutive data points, excluding the very first data point at ~ 0 min.

Figure S13: Figure showing how the average conversion was calculated from the kinetic measurements. This example shows the calculation of average conversion at 200 mbar H_2 and 100 mbar *n*-heptane at 703 K and atmospheric pressure.

Secondly, for the determination of the H_2 reaction order the average valve of the very first three consecutive data points, excluding the very first one, was considered for the calculation of the reaction rate (i.e., average valve of 2nd, 3rd, and 4th data point in Figure S13). Figure S14 shows the calculation of the reaction rate ($mol_{heptane} g_{Pt}^{-1} h^{-1}$) and how it is reflected in H_2 reaction order determination plot.

Exp.	P_{H2} (bar)	Avg. Conversion (%)	Rate ($mol_{Heptane}\ gPt^{-1}\ hr^{-1}$)	ln(Rate) (-)	ln(P_{H2}) (-)
Ga-Pt/AlOx SCALMS (Pt = 0.08 wt.%)					
224	0.2	5.89%	1.09	0.09	-1.61
228	0.2	6.07%	1.12	0.12	-1.61

Exp.	P_{H2} (bar)	Avg. Conversion (%)	Rate ($mol_{Heptane}\ gPt^{-1}\ hr^{-1}$)	ln(Rate) (-)	ln(P_{H2}) (-)
Pt/AlOx (Pt = 0.12 wt.%)					
198	0.2	5.63%	0.71	-0.34	-1.61
202	0.2	5.72%	0.72	-0.33	-1.61

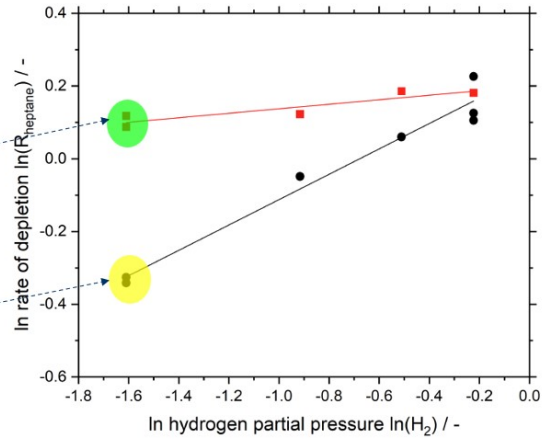

Figure S14: Figure showing how the average conversion was calculated is reflected in the reaction order determination plot. This example shows the calculation of reaction rate at 200 mbar H_2 and 100 mbar *n*-heptane at 703 K and atmospheric pressure and how it is reflected in H_2 reaction order determination plot.

References

1 Olafadehan, O. A., Susu, A. A. & Jaiyeola, A. Mechanistic Kinetic Models for n-Heptane Reforming on Platinum/Alumina Catalyst. *Pet Sci Technol* **26**, 1459-1480 (2008). https://doi.org:10.1080/10916460701675157

2 González-Marcos, M. P., Iñarra, B., Guil, J. M. & Gutiérrez-Ortiz, M. A. Development of an industrial characterisation method for naphtha reforming bimetallic Pt-Sn/Al_2O_3 catalysts through n-heptane reforming test reactions. *Catal Today* **107-108**, 685-692 (2005). https://doi.org:10.1016/j.cattod.2005.07.052

3 Van Trimpont, P. A., Marin, G. B. & Froment, G. F. Reforming of C7 hydrocarbons on a sulfided commercial platinum/alumina catalyst. *Ind Eng Chem Res* **27**, 51-57 (1988). https://doi.org:10.1021/ie00073a012

4 Yu, N., Long, J., Zhou, H., Ma, A. & Dai, Z. Simulation of the Reaction Mechanism of Dehydrogenation of n-Heptane to Produce Olefins. *Acta Petrol Sin* **32**, 437-443 (2016). https://doi.org:10.3969/j.issn.1001-8719.2016.03.001

5 Liu, K., Fung, S. C., Ho, T. C. & Rumschitzki, D. S. Heptane Reforming over Pt–Re/Al2O3: Reaction Network, Kinetics, and Apparent Selective Catalyst Deactivation. *J Catal* **206**, 188-201 (2002). https://doi.org:10.1006/jcat.2001.3485

6 Tregubenko, V. Y., Vinichenko, N. V., Paukshtis, E. A., Udras, I. E. & Belyi, A. S. in *AIP Conference Proceedings* Vol. 2141 020015 (2019).

7 Van Trimpont, P. A., Marin, G. B. & Froment, G. F. Kinetics of the reforming of C7 hydrocarbons on a commercial PtRe/Al_2O_3 catalyst. *Appl Catal* **24**, 53-68 (1986). https://doi.org:10.1016/S0166-9834(00)81257-9

8 Saberi, M. A. & Le Van Mao, R. Comparative study of the kinetic behavior of the bifunctional and trifunctional catalysts in the hydroisomerization of n-heptane. *Appl Catal A Gen* **242**, 139-150 (2003). https://doi.org:10.1016/s0926-860x(02)00522-7

9 Usman, M. R. & Alotaibi, F. M. Unified kinetics of n-heptane hydroisomerisation over various Pt/zeolite catalysts. *Prog React Kinet Mech* **41**, 177-192 (2016). https://doi.org:10.3184/146867816x14646899008350

10 Demirci, Ü. B. & Garin, F. Kinetic study of n-heptane conversion on sulfated zirconia-supported platinum catalyst: the metal–proton adduct is the active site. *J Mol Catal A Chem*

188, 233-243 (2002). https://doi.org:10.1016/S1381-1169(02)00337-0

11 Parsafard, N., Peyrovi, M. H. & Rashidzadeh, M. Experimental and kinetic study of n-heptane isomerization on nanoporous Pt-(Re, Sn)/HZSM5-HMS catalysts. *Chinese J Catal* **37**, 1477-1486 (2016). https://doi.org:10.1016/s1872-2067(15)61114-7

12 Holló, A., Hancsók, J. & Kalló, D. Kinetics of hydroisomerization of C_5–C_7 alkanes and their mixtures over platinum containing mordenite. *Appl Catal A Gen* **229**, 93-102 (2002). https://doi.org:10.1016/S0926-860X(02)00018-2

13 Peyrovi, M. H., Parsafard, N. & Peyrovi, P. Influence of Zirconium Addition in Platinum–Hexagonal Mesoporous Silica (Pt-HMS) Catalysts for Reforming of n-Heptane. *Ind Eng Chem Res* **53**, 14253-14262 (2014). https://doi.org:10.1021/ie5024244

14 Liers, J., Meusinger, J. & Reschetilowski, W. Comparison of cracking and hydrocraking ofn-heptane on H-ZSM-5 catalysts. *Chem Eng Technol* **16**, 422-428 (1993). https://doi.org:10.1002/ceat.270160611

15 Remy, M. J. *et al.* Dealuminated H-Y Zeolites: Relation between Physicochemical Properties and Catalytic Activity in Heptane and Decane Isomerization. *J Phys Chem* **100**, 12440-12447 (1996). https://doi.org:10.1021/jp953006x

16 Iglesla, E., Barton, D. G., Biscardi, J. A., Gines, M. J. L. & Soled, S. L. Bifunctional pathways in catalysis by solid acids and bases. *Catal Today* **38**, 339-360 (1997). https://doi.org:0.1016/S0920-5861(97)81503-7